January 3, 2025

McCloud River Shasta Dam, California

2024 Topobathymetric Lidar and Imagery Technical Data Report

Prepared For:

Anchor QEA, LLC
Greg Stewart
14 N. Wenatchee Ave, Suite 139
Wenatchee, WA 98801

Prepared By:

NV5 Corvallis
1100 NE Circle Blvd, Ste. 126
Corvallis, OR 97330
PH: 541-752-1204

TABLE OF CONTENTS

Cover Photo: A view looking north along the McCloud River. The image was taken by the survey team at NV5.

LIST OF FIGURES

LIST OF TABLES

INTRODUCTION

This photo, taken by NV5 acquisition staff, shows a frog on some rocks within the project AOI site.

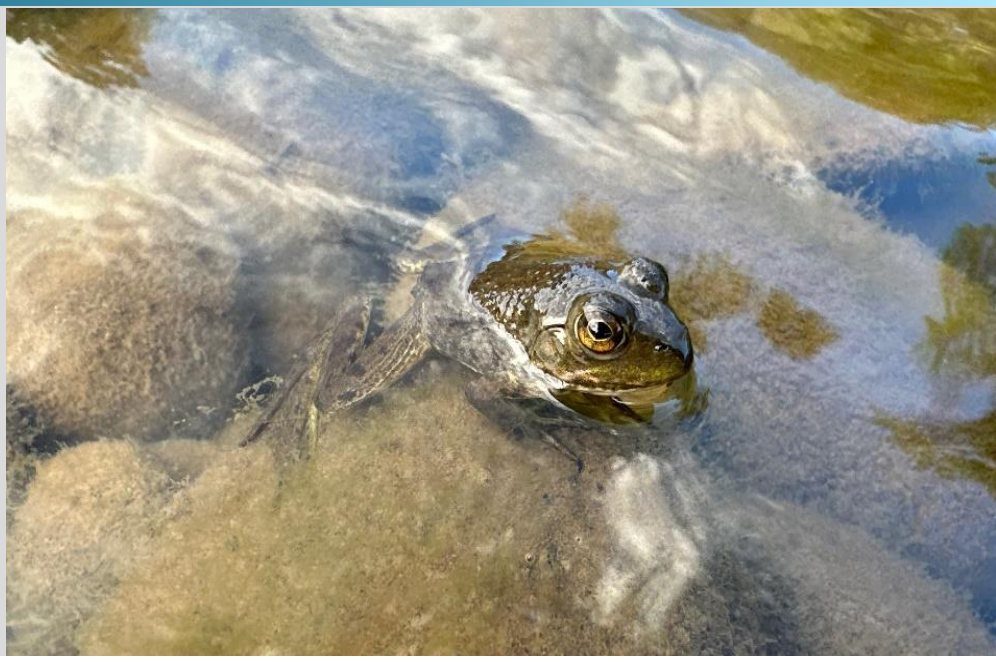

In August 2024, NV5 was contracted by Anchor QEA, LLC (Anchor) to collect topobathymetric Light Detection and Ranging (lidar) data and co-acquired digital imagery in the fall of 2024 for the McCloud River Shasta Dam project in California. The McCloud River Shasta Dam project areas of interest include portions of the McCloud River, Dry Creek, Cow Creek and Little Cow Creek located in Shasta County, California. Traditional near-infrared (NIR) lidar was fully integrated with green wavelength return (bathymetric) lidar data in order to provide a seamless topobathymetric lidar dataset. Data were collected to aid Anchor in assessing the channel morphology and topobathymetric surface of the McCloud River Shasta Dam and nearby creeks to support a wildlife study focused on Salmon habitats above Lake Shasta Dam.

This report accompanies the delivered topobathymetric lidar data and imagery, and documents contract specifications, data acquisition procedures, processing methods, and analysis of the final dataset including lidar accuracy, depth penetration, and density. Acquisition dates and acreage are shown in Table 1, a complete list of contracted deliverables provided to Anchor is shown in Table 3 with the coordinate reference system information for these deliverables shown in Table 2, and the project extent is shown in Figure 1.

Table 1: Acquisition dates, acreage, and data types collected on the McCloud River Shasta Dam sites

Project Site	Contracted Acres	Buffered Acres	Aerial Acquisition Dates	Data Type
McCloud River Shasta Dam, California	2,258	3,422	10/6/2024 & 10/7/2024	• Topobathymetric Lidar • 3 band (RGB) Digital Imagery

Deliverable Products

Table 2: Deliverable product coordinate reference system information

Projection	Horizontal Datum	Vertical Datum	Units
California State Plane Zone 1	NAD83 (2011)	NAVD88 (GEOID18)	U.S. Survey Feet

Table 3: Lidar and imagery products delivered for the McCloud River Shasta Dam site

Product Type	File Type	Product Details
Points	LAS v.1.4 (*.las)	• All Classified Returns
Rasters	1.5 foot Resolution GeoTIFFs (*.tif)	• Void-Interpolated Topobathymetric Bare Earth Digital Elevation Model (DEM) • Void-Clipped Topobathymetric Bare Earth Digital Elevation Model (DEM) • Highest Hit Digital Surface Model (DSM) • Green Sensor Intensity Images • NIR Sensor Intensity Images
Vectors	Shapefiles (*.shp)	• Buffered Project Boundary • Tile Index • Bathymetric Coverage/Void Polygon • 2D Hydrology Breaklines
Digital Imagery	0.5 foot GeoTIFFs (*.tif)	• Tiled Imagery Mosaics
Digital Imagery	0.5 foot Compression (*.sid)	• AOI Imagery Mosaic
Metadata	Extensible Markup Language (*.xml)	• FGDC Metadata
Reports	Adobe Acrobat (*.pdf)	• Lidar and Imagery Technical Data Report

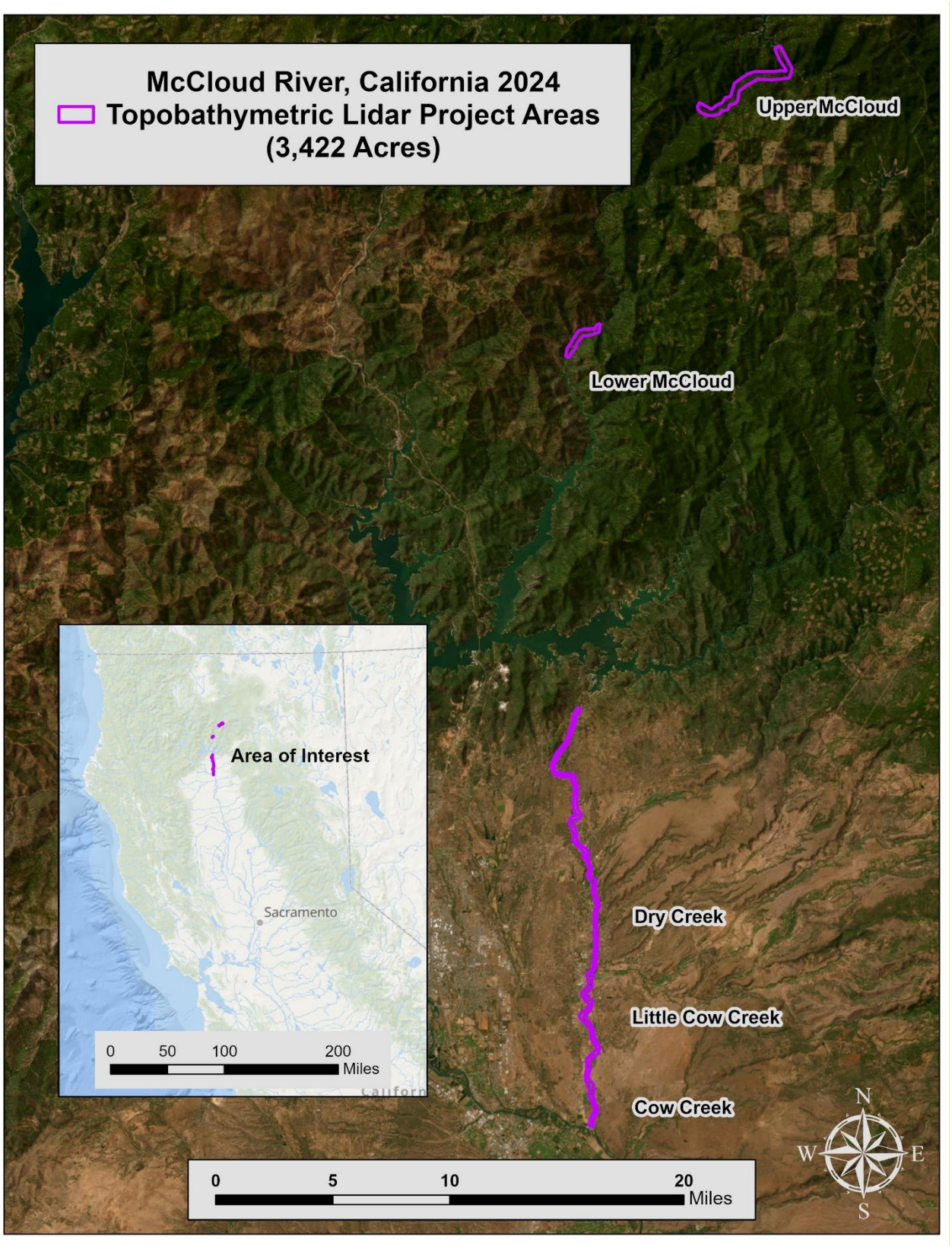

Figure 1: Location map of the McCloud River Shasta Dam project in California

ACQUISITION

NV5's Cessna Grand Caravan

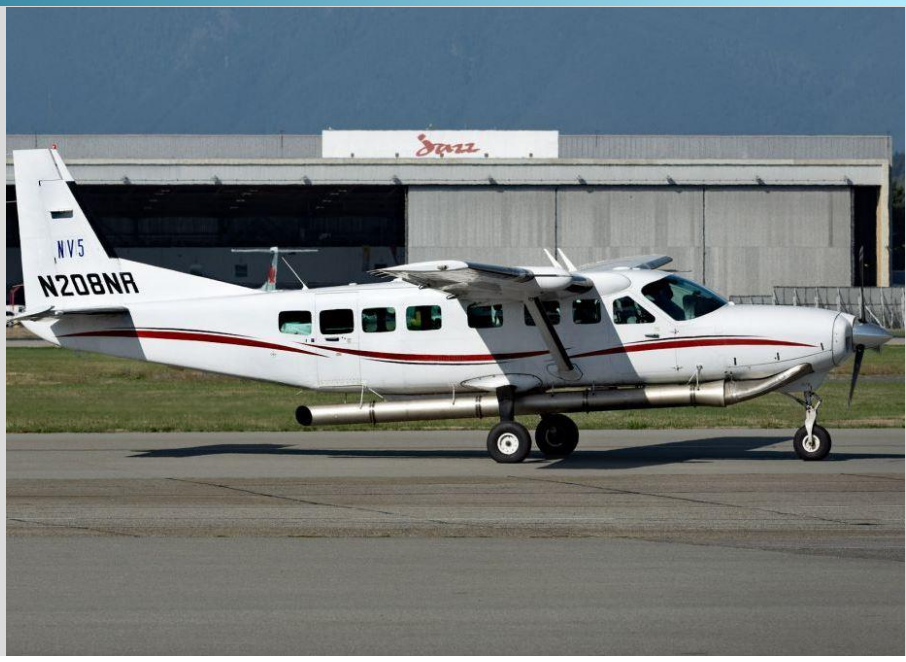

Planning

In preparation for data collection, NV5 reviewed the project area and developed a specialized flight plan to ensure complete coverage of the McCloud River Shasta Dam Lidar study area at the target combined point density of ≥ 8 points/m^2 (0.74 points/ft^2). Acquisition parameters including orientation relative to terrain, flight altitude, pulse rate, scan angle, and ground speed were adapted to optimize flight paths and flight times while meeting all contract specifications. Figure 5 shows these optimized flight paths and dates.

Factors such as satellite constellation availability and weather windows must be considered during the planning stage. Any weather hazards or conditions affecting the flight were continuously monitored due to their potential impact on the daily success of airborne and ground operations. In addition, logistical considerations including private property access, potential air space restrictions, channel flow rates (Figure 2 and Figure 3), and water clarity (Figure 4) were reviewed.

Secchi Depth Readings

In order to assess water clarity conditions prior to and during lidar and digital imagery collection, NV5 collected and Secchi depth readings. Readings were collected at three locations throughout the project site between October 7th and October 8th, 2024. Turbidity observations were recorded three times to confirm measurements. Table 4 below provides turbidity and Secchi depth results per site on each day of data collection. Table 4 below provides Secchi depth results per site on each day of data collection. A true Secchi depth reading is where the Secchi depth reaches extinction. However, because of safety concerns and accessibility, some Secchi depth readings were noted to have reached the bottom surface of the riverbed.

Table 4: 2024 water clarity observations for lidar flights

Date	Site	Latitude	Longitude	Turbidity Read 1 (NTU)	Turbidity Read 2 (NTU)	Turbidity Read 3 (NTU)	*Secchi Depth (m)
10/7	1	40° 33' 19.43"	-122° 13' 51.97"	4.80	5.63	4.72	0.76
10/7	2	40° 35' 30.67"	-122° 13' 35.85"	3.12	1.76	1.73	0.46
10/8	3	40° 33' 19.77"	-122° 13' 52.33"	4.60	4.39	3.24	1.98

** Measurement is depth to the bottom surface due to observational depth limitations*

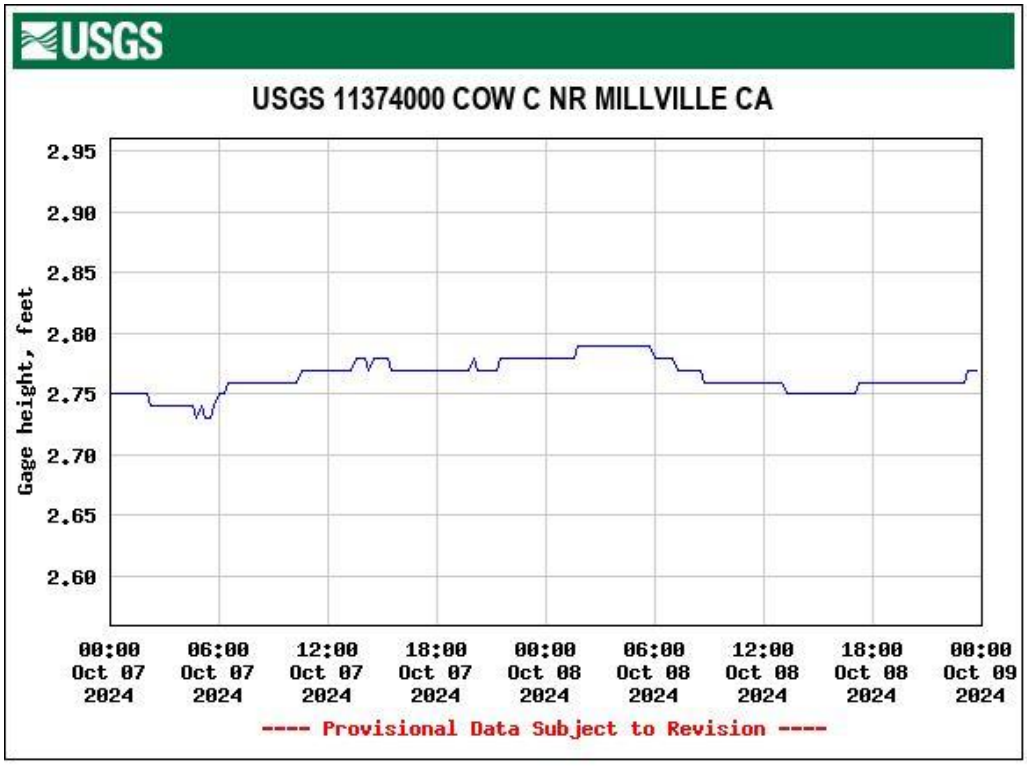

Figure 2: USGS Station 11374000 gage height along Cow Creek at the time of lidar acquisition.

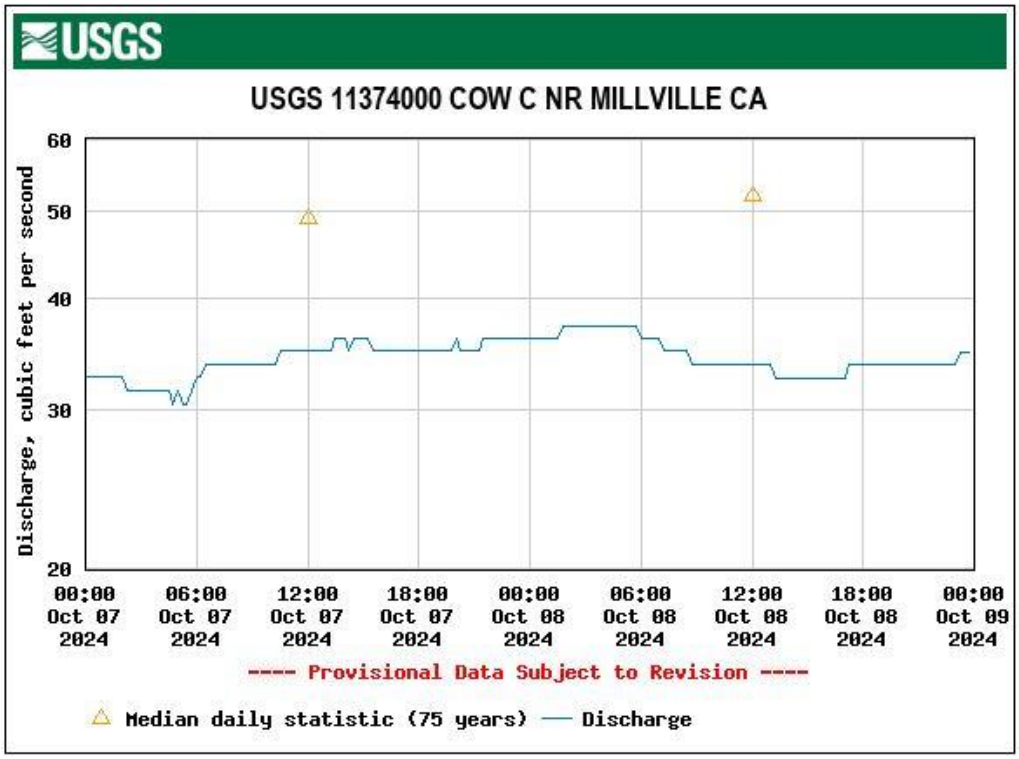

Figure 3: USGS Station 11374000 flow rates along Cow Creek at the time of lidar acquisition.

Figure 4: This photo was taken by NV5 acquisition staff displays water clarity conditions near the Shasta Dam site.

Airborne Lidar Survey

The lidar survey was accomplished using a Riegl VQ-880-GII green laser system mounted in a Cessna Grand Caravan. The Riegl VQ-880-GII boasts a high repetition pulse rate (up to 550 kHz), high scanning speed, small laser footprint, and wide field of view which allows for seamless collection of high resolution data of both topographic and bathymetric surfaces. The green wavelength (ʎ=532 nm) laser is capable of collecting high resolution topography data, as well as penetrating the water surface with minimal spectral absorption by water. The Riegl VQ-880-GII contains an integrated NIR laser (ʎ=1064 nm) that adds additional topography data and aids in water surface modeling. The Riegl VQ-880-GII laser system can record unlimited range measurements (returns) per pulse, however a maximum of 15 returns can be stored due to LAS v1.4 file limitations. Due to elevational changes in the terrain, flightlines over the McCloud River areas were conducted at a higher survey altitude. Table 5 summarizes the settings used to yield an average pulse density of ≥8 pulses/m^2 over the McCloud River Shasta Dam project. Figure 5 shows the flightlines acquired using these lidar specifications.

All areas were surveyed with an opposing flight line side-lap of ≥ 60% (≥ 120% overlap) in order to reduce laser shadowing and increase surface laser painting. To accurately solve for laser point position (geographic coordinates x, y, and z), the positional coordinates of the airborne sensor and the orientation of the aircraft to the horizon (attitude) were recorded continuously throughout the lidar data collection mission. Position of the aircraft was measured twice per second (2 Hz) by an onboard differential GPS unit, and aircraft attitude was measured 200 times per second (200 Hz) as pitch, roll, and yaw (heading) from an onboard inertial measurement unit (IMU). To allow for post-processing correction and calibration, aircraft and sensor position and attitude data are indexed by GPS time.

Table 5: Lidar specifications and aerial survey settings

Parameter	Green Laser	NIR Laser
Acquisition Dates	10/6/2024, 10/7/2024	10/6/2024, 10/7/2024
Aircraft Used	Cessna Grand Caravan	Cessna Grand Caravan
Sensor	Riegl	Riegl
Laser Channel	VQ-880GII-Green	VQ-880GII-IR
Maximum Returns	8	12
Resolution/Density	Average 8 points/m²	Average 8 points/m²
Nominal Pulse Spacing	0.35 m	0.35 m
Survey Altitude (AGL)	400 - 1300 m	400 - 1300 m
Survey speed	120 - 145 knots	120 - 145 knots
Field of View	40°	42°
Mirror Scan Rate	80 Lines per Second	Uniform Point Spacing
Target Pulse Rate	200 kHz	150 - 300 kHz
Pulse Length	1.5 ns	3 ns
Laser Pulse Footprint Diameter	28 – 91 cm	12 - 39 cm
Central Wavelength	532 nm	1064 nm
Pulse Mode	MTA (multiple times around)	MTA (multiple times around)
Beam Divergence	0.7 mrad	0.3 mrad
Swath Width	291 - 946 m	307 - 998 m
Swath Overlap	60%	60%
Intensity	16-bit	16-bit
Vertical Accuracy	$RMSE_Z \leq 10$ cm	$RMSE_Z \leq 10$ cm

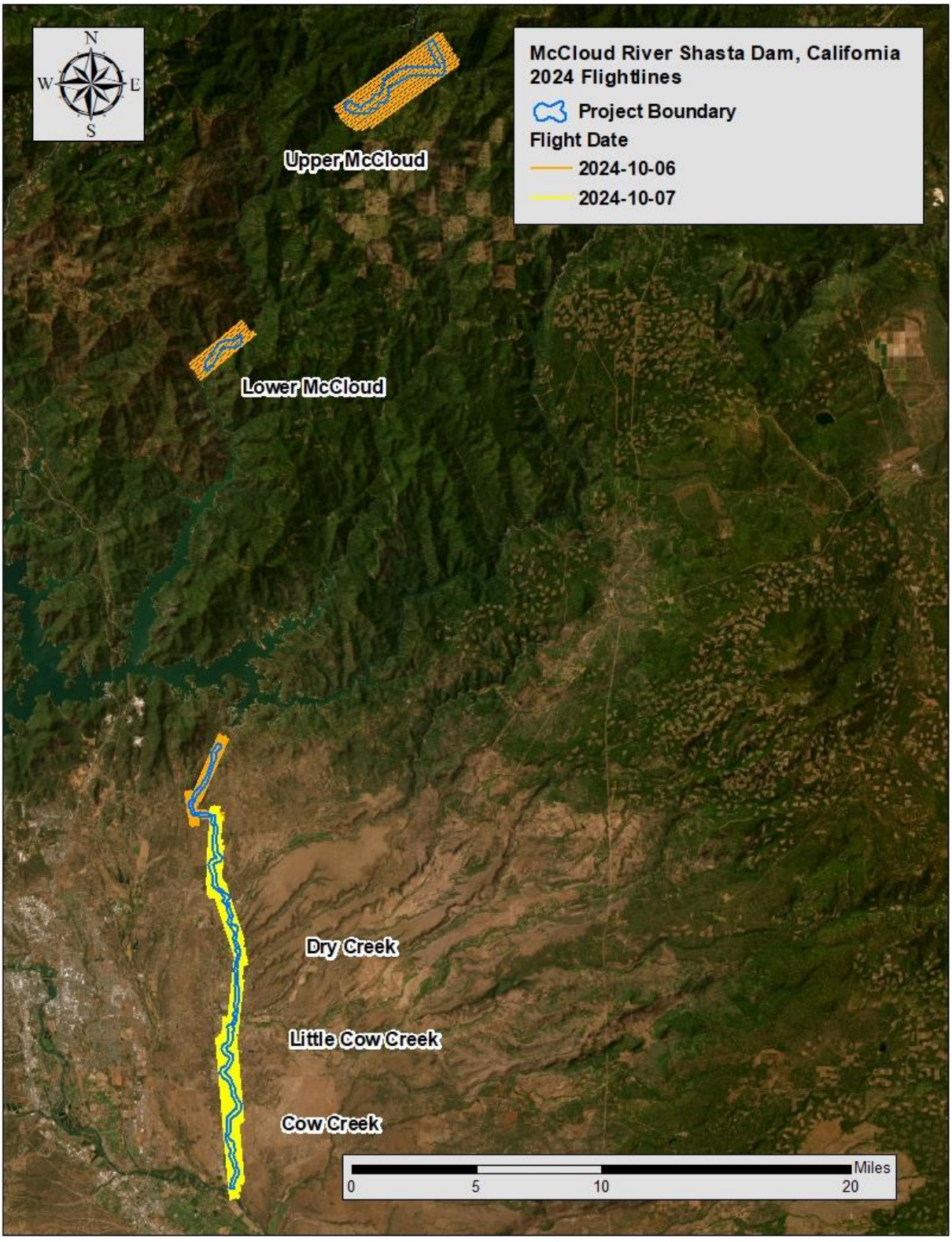

Figure 5: Flightlines map

Digital Imagery

Aerial imagery was co-acquired (with the lidar) using a PhaseOne iXM-RS150F digital camera (Table 6). The PhaseOne is a medium format aerial mapping camera which collects imagery in three spectral bands (Red, Green, Blue).

Table 6: Camera manufacturer's specifications for a PhaseOne iXM-RS150F

Parameter	PhaseOne iXM-RS150F Specification
Focal Length	70 mm
Spectral Bands	Red, Green, Blue
Pixel Size	3.76 µm
Image Size	14,204 x 10,652 pixels
Frame Rate	GPS triggered
FOV	42° x 32°
Data Format	8bit TIFF

For the McCloud River Shasta Dam site, 3,279 images were collected in 77 flightlines with 60% along track overlap and 30% sidelap between frames. The acquisition flight parameters were designed to yield a native pixel resolution of ≤ 6 inches (15 cm). Orthophoto specifications particular to the McCloud River Shasta Dam project are in Table 7.

Table 7: Project-specific orthophoto specifications

Parameter	Digital Orthophotography Specification
Ground Sampling Distance (GSD)	≤ 6 inch pixel size
Along Track Overlap	≥ 60%
Cross Track Overlap	≥ 30%
Height Above Ground Level (AGL)	400 - 1300 m
GPS PDOP	≤3.0
GPS Satellite Constellation	≥6

Ground Survey

Ground control surveys, including monumentation, aerial targets, and ground survey points (GSPs), were conducted to support the airborne acquisition. Ground control data were used to geospatially correct the aircraft positional coordinate data and to perform quality assurance checks on final lidar data and orthoimagery products.

NV5-Established Monument – MCCLOUD_02

Base Stations

Base stations were used for collecting ground survey points using real time kinematic (RTK), fast static (FS), and post processed kinematic (PPK) survey techniques.

Base station locations were selected with consideration for satellite visibility, field crew safety, and optimal location for GSP coverage. NV5 utilized one permanent base station from the California Surveying & Drafting Supply (CSDS) real-time network (RTN), two new monuments, and one existing NGS monument for the McCloud River Shasta Dam Lidar project (Table 8, Figure 7). New monuments were set using 6" mag hub nails with green survey washers (Table 8). NV5's professional land surveyor, Evon Silvia (CA PLS#9401), oversaw and certified the ground survey.

Table 8: Base Station positions for the acquisition coordinates are on the NAD83 (2011) datum, epoch 2010.00

Monument ID	Latitude	Longitude	Ellipsoid (meters)	Owner	Type
MCCLOUD_01	40° 56' 25. 37252 "	-122° 14' 45. 42726"	304.878	NV5	Mag
MCCLOUD_02	41° 07' 56. 76471"	-122° 04' 16.93029 "	797.450	NV5	Mag
P349	40° 43' 51.89424"	-122° 19' 09.60929"	275.859	NGS	CORS
RD1L	40° 31' 55.15292"	-122° 17' 01.75429"	132.813	CSDS	CORS

NV5 utilized static Global Navigation Satellite System (GNSS) data collected at 1 Hz recording frequency for each base station. During post-processing, the static GNSS data was triangulated with nearby Continuously Operating Reference Stations (CORS) using the Online Positioning User Service (OPUS[1]) for precise positioning. Multiple independent sessions over the same monument were processed to confirm antenna height measurements and to refine position accuracy.

Monuments were established according to the national standard for geodetic control networks, as specified in the Federal Geographic Data Committee (FGDC) Geospatial Positioning Accuracy Standards

[1] OPUS is a free service provided by the National Geodetic Survey to process corrected monument positions: OPUS website

for geodetic networks.[2] This standard provides guidelines for classification of monument quality at the 95% confidence interval as a basis for comparing the quality of one control network to another. The monument rating for this project is shown in Table 9.

Table 9: Federal Geographic Data Committee monument rating for network accuracy

Direction	Rating
1.96 * St Dev $_{NE}$:	0.020 m
1.96 * St Dev $_{z}$:	0.020 m

For the McCloud River Shasta Dam Lidar project, the monument coordinates contributed no more than 2.8 cm of positional error to the geolocation of the final ground survey points and lidar, with 95% confidence.

Ground Survey Points (GSPs)

Ground survey points were collected using real time kinematic (RTK), post-processed kinematic (PPK), and fast-static (FS) survey techniques. For RTK surveys, a roving receiver receives corrections from a nearby base station or Real-Time Network (RTN) via radio or cellular network, enabling rapid collection of points with relative errors less than 1.5 cm horizontal and 2.0 cm vertical. PPK and FS surveys compute these corrections during post-processing to achieve comparable accuracy. RTK and PPK surveys record data while stationary for at least five seconds, calculating the position using at least three one-second epochs. FS surveys record observations for up to fifteen minutes on each GSP to support longer baselines. All GSP measurements were made during periods with a Position Dilution of Precision (PDOP) of ≤ 3.0 with at least six satellites in view of the stationary and roving receivers. See Table 10 for NV5 ground survey equipment information.

GSPs were collected in areas where good satellite visibility was achieved on paved roads and other hard surfaces such as gravel or packed dirt roads. GSP measurements were not taken on highly reflective surfaces such as center line stripes or lane markings on roads due to the increased noise seen in the laser returns over these surfaces. GSPs were collected within as many flightlines as possible; however, the distribution of GSPs depended on ground access constraints and monument locations and may not be equably distributed throughout the study area (Figure 7).

Table 10: NV5 ground survey equipment identification

Receiver Model	Antenna	OPUS Antenna ID	Use
Trimble R750	Zephyr Model 3 GNSS	TRM115000.10	Static
Trimble R12	Integrated Antenna	TRMR12	Rover

[2] Federal Geographic Data Committee, Geospatial Positioning Accuracy Standards (FGDC-STD-007.2-1998). Part 2: Standards for Geodetic Networks, Table 2.1, page 2-3: FGDC Standards Website

Aerial Targets

Air target points (ATP) were collected throughout the project area prior to imagery acquisition to refine the exterior orientation parameters of the camera and conduct the accuracy assessment of the final orthophoto product (Figure 6). ATPs are typically collected over hard surface ground features or temporary vinyl chevrons. Hard surface points consist of high contrast, road markings such as stop bars and turn arrows and cement corners. Each ATP was surveyed using Fast Static (FS) or RTK techniques.

Figure 6: Examples of aerial targets

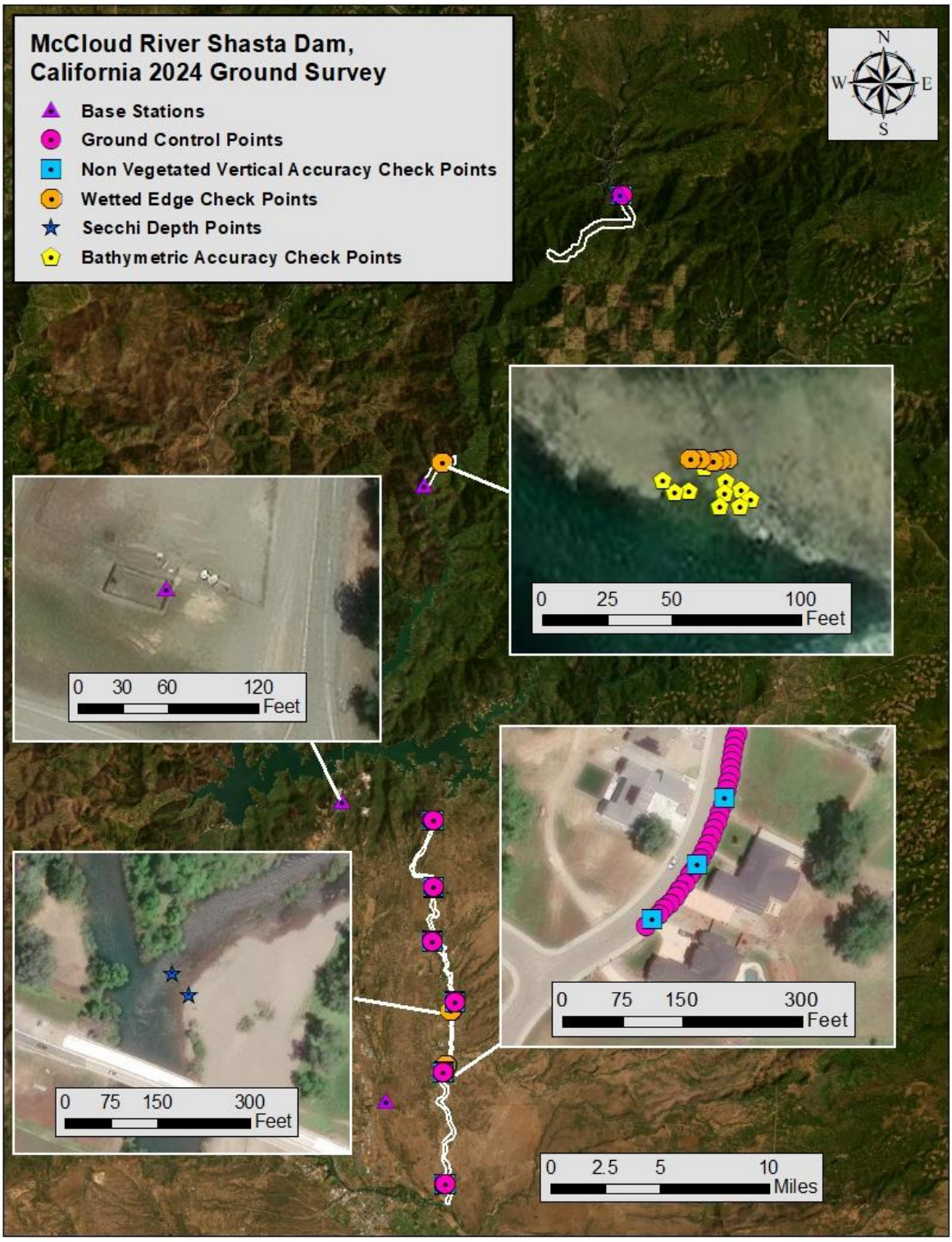

Figure 7: Ground survey location map

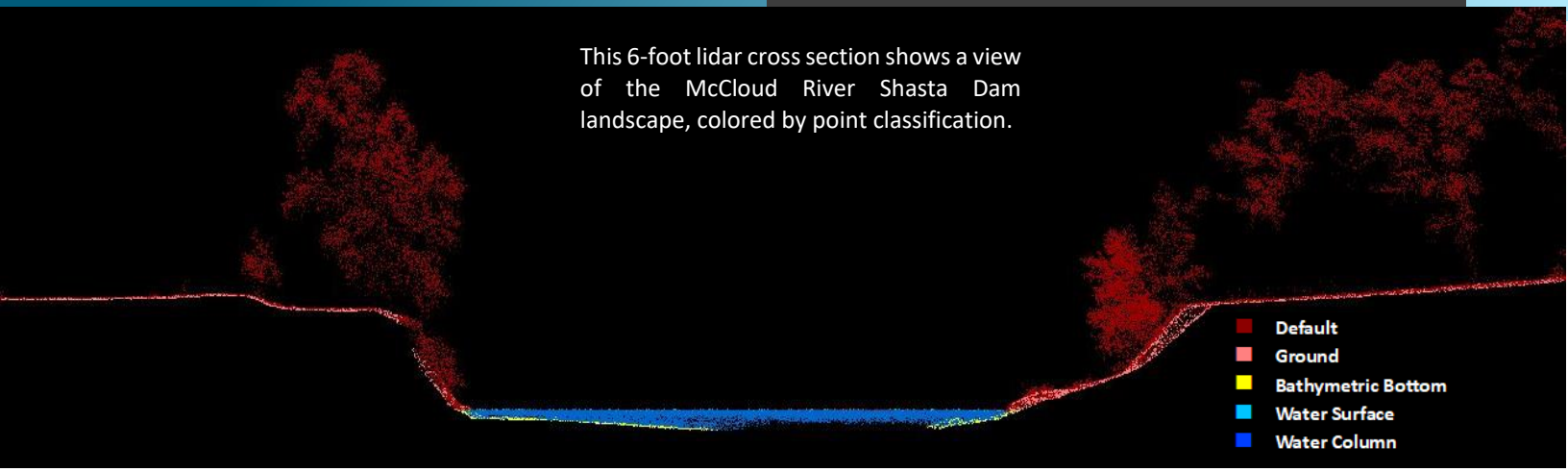

This 6-foot lidar cross section shows a view of the McCloud River Shasta Dam landscape, colored by point classification.

Topobathymetric Lidar Data

Upon completion of data acquisition, NV5 processing staff initiated a suite of automated and manual techniques to process the data into the requested deliverables. Processing tasks included GPS control computations, smoothed best estimate trajectory (SBET) calculations, kinematic corrections, calculation of laser point position, sensor and data calibration for optimal relative and absolute accuracy, and lidar point classification (Table 11).

Riegl's RiProcess software was used to facilitate bathymetric return processing. Once bathymetric points were differentiated, they were spatially corrected for refraction through the water column based on the angle of incidence of the laser. NV5 refracted water column points using NV5's proprietary LAS processing software, Las Monkey. The resulting point cloud data was classified using both manual and automated techniques. Processing methodologies were tailored for the landscape. Brief descriptions of these tasks are shown in Table 12.

Table 11: ASPRS LAS classification standards applied to the McCloud River Shasta Dam dataset

Classification Number	Classification Name	Classification Description
1	Default/Unclassified	Laser returns that are not included in the ground class, composed of vegetation and anthropogenic features.
2	Ground	Laser returns that are determined to be ground using automated and manual cleaning algorithms.
7	Noise	Laser returns that are often associated with birds, scattering from reflective surfaces, or artificial points below the ground surface.
9	Water	NIR Laser returns that are determined to be water using automated and manual cleaning algorithms.
17	Bridge	Bridge decks.
40	Bathymetric Bottom	Refracted green laser returns that fall within the water's edge breakline which characterize the submerged topography.
41	Water Surface	Green laser returns that are determined to be water surface points using automated and manual cleaning algorithms.
45	Water Column	Refracted green sensor returns that are determined to be water using automated and manual cleaning algorithms.

Table 12: Lidar processing workflow

Lidar Processing Step	Software Used
Resolve kinematic corrections for aircraft position data using kinematic aircraft GPS and static ground GPS data. Develop a smoothed best estimate of trajectory (SBET) file that blends post-processed aircraft position with sensor head position and attitude recorded throughout the survey.	POSPac MMS v.8.9
Calculate laser point position by associating SBET position to each laser point return time, scan angle, intensity, etc. Create raw laser point cloud data for the entire survey in *.las (ASPRS v. 1.4) format. Convert data to orthometric elevations by applying a geoid correction.	RiUnite v1.0.3
Import raw laser points into manageable blocks to perform manual relative accuracy calibration and filter erroneous points. Classify ground points for individual flight lines.	TerraScan v.19.005
Using ground classified points per each flight line, test the relative accuracy. Perform automated line-to-line calibrations for system attitude parameters (pitch, roll, heading), mirror flex (scale), and GPS/IMU drift. Calculate calibrations on ground classified points from paired flight lines and apply results to all points in a flight line. Use every flight line for relative accuracy calibration.	StripAlign v.2.2.4
Apply refraction correction to all subsurface returns.	Las Monkey v.2.6.9 (NV5 proprietary)
Classify resulting data to ground and other client designated ASPRS classifications (Table 11). Assess statistical absolute accuracy via direct comparisons of ground classified points to ground control survey data.	TerraScan v.19.005 TerraModeler v.19.003
Generate bare earth models as triangulated surfaces. Generate highest hit models as a surface expression of all classified points. Export all surface models as Cloud-Optimized GeoTIFFs, at a 1.5 foot pixel resolution.	Las Product Creator 4.0 (NV5 proprietary software) ArcMap v. 10.8
Export intensity images as cloud optimized GeoTIFFs at a 1.5 foot pixel resolution.	Las Product Creator 4.0 (NV5 proprietary software)

Bathymetric Refraction

Green lidar pulses that enter the water column must have their position corrected for refraction of the light beam as it passes through the water and its resulting decreased speed. NV5 has developed proprietary software (Las Monkey) to perform this processing based on Snell's law. The first step is to develop a water surface model (WSM) covering all submerged returns within the project boundary. The water surface model used for refraction is generated from points within the wetted edge breaklines that include NIR points representing the water surface as well as elevations sampled from the ground at the water's edge. Points are filtered and edited to obtain the most accurate representation of the water surface and are used to create a water surface model TIN. A TIN model is preferable to a raster-based water surface model in obtaining the most accurate angle of incidence during refraction.

Once the WSM is generated, the Las Monkey refraction software then intersects the partially submerged green pulses with the WSM to determine the angle of incidence with the water surface and the submerged component of the pulse vector. This provides the information necessary to correct the position of underwater points by adjusting the submerged vector length and orientation. After refraction, the points are compared against bathymetric checkpoints to assess accuracy.

The water surface models used for refraction are generated using elevation information derived from the NIR channel to inform where the green water surface level is located, and then water surface points are classified for both the forward and reverse look directions of the green scanner. Points are filtered and edited to obtain the most accurate representation of the water surface and are used to create a water surface model for each flight line and look direction. Water surface classification and modeling is processed on each flight line to accommodate water level changes due to riverine and temporal changes in water surface. Each look direction (forward and reverse) is modeled separately to correctly model short duration time dependent surface changes that change between the times that each look direction records a unique location. The water surface model created is raster based with an associated surface normal vector to obtain the most accurate angle of incidence during refraction. The refraction processing is done using RiHydro tools which is a component running within Riegl's RiProcess software.

Lidar Derived Products

Because hydrographic laser scanners penetrate the water surface to map submerged topography, this affects how the data should be processed and presented in derived products from the lidar point cloud. The following section discusses certain derived products that vary from the traditional (NIR) specification and delivery format.

Topobathymetric DEMs

Bathymetric bottom returns can be limited by depth, water clarity, and bottom surface reflectivity. Water clarity and turbidity affects the depth penetration capability of the green wavelength laser with returning laser energy diminishing by scattering throughout the water column. Additionally, the bottom surface must be reflective enough to return remaining laser energy back to the sensor at a detectable level. Although the predicted depth penetration range of the Riegl VQ-880-GII sensor is 1.5 Secchi depths on brightly reflective surfaces, it is not unexpected to have no bathymetric bottom returns in turbid or non-reflective areas.

As a result, creating digital elevation models (DEMs) presents a challenge with respect to interpolation of areas with no returns. Traditional DEMs are "unclipped," meaning areas lacking ground returns are interpolated from neighboring ground returns (or breaklines in the case of hydro-flattening), with the

assumption that the interpolation is close to reality. In bathymetric modeling, these assumptions are prone to error because a lack of bathymetric returns can indicate a change in elevation that the laser can no longer map due to increased depths. The resulting void areas may suggest greater depths, rather than similar elevations from neighboring bathymetric bottom returns. Therefore, NV5 created a water polygon with bathymetric coverage to delineate areas with successfully mapped bathymetry. This shapefile was used to control the extent of the delivered clipped topobathymetric model to avoid false triangulation (interpolation from TIN'ing) across areas in the water without bathymetric bottom returns.

Intensity Images

The first returns of all valid point classes were used for both the green and NIR sensors in order to create intensity images. With bathymetric lidar a more detailed and informative intensity image can be created by using all or selected point classes, rather than relying on return number alone. If intensity information of the bathymetry is the primary goal, water surface and water column points can be excluded. However, water surface and water column points often contain potentially useful information about turbidity and submerged but unclassified features such as vegetation. For the McCloud River Shasta Dam project, NV5 created one set of intensity images from NIR laser first returns, as well as one set of intensity images from green laser returns (Figure 8).

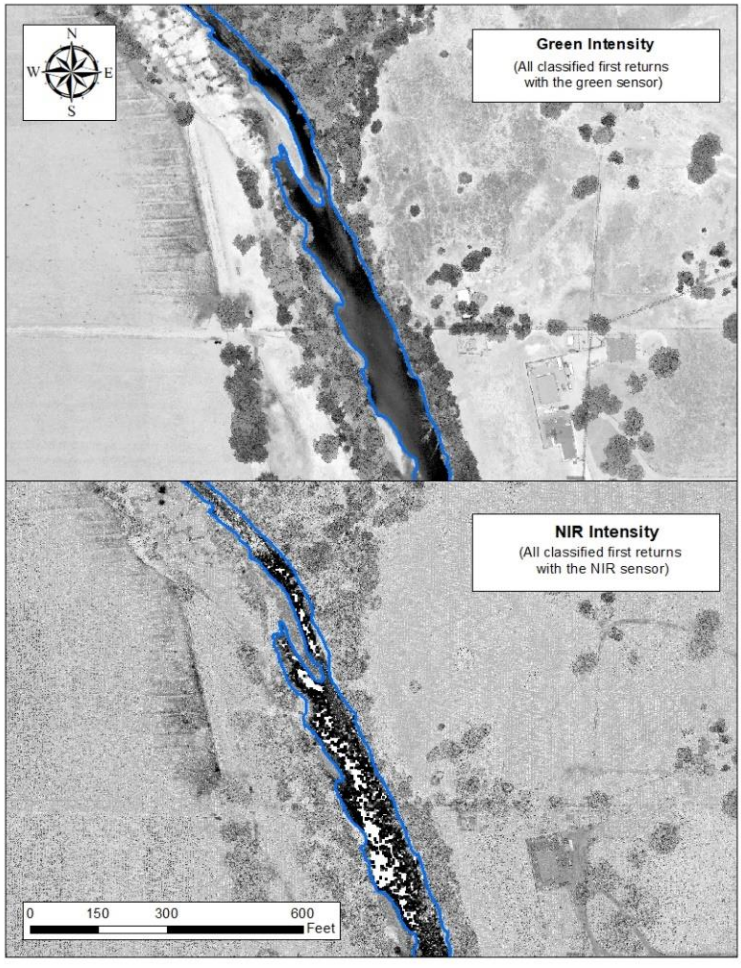

Figure 8: A comparison of intensity images from green and NIR first returns in the McCloud River Shasta Dam area

Digital Imagery

As with the NIR lidar, the collected digital photographs went through multiple processing steps to create final orthophoto products. Initially, raw images were geometrically corrected to remove lens distortion and output as 3band tiff images. Photo position and orientation, as camera exterior orientations (EO), were then calculated by linking the time of image capture to the smoothed best estimate of trajectory (SBET) file created during lidar post-processing. Within Inpho Match AT, an automated aerial triangulation was performed to refine EO parameters and adjust the photo block to ground control.

Adjusted images were orthorectified using the lidar-derived ground model to remove displacement effects from topographic relief inherent in the imagery. The resulting orthophotos were mosaicked within Inpho's OrthoVista using automated seamline generation and applying global color-balancing to the block. The final mosaics were inspected and edited for seam cutlines across above ground features such as buildings and other man-made features. The processing workflow for orthophotos is summarized in Table 13.

Table 13: Orthophoto processing workflow

Orthophoto Processing Step	Software Used
Resolve GPS kinematic corrections for the aircraft position data using kinematic aircraft GPS (collected at 2 Hz) and Applanix PPRTX data.	POSPac MMS v9
Develop a smooth best estimate trajectory (SBET) file that blends post-processed aircraft position with attitude data. Sensor heading, position, and attitude are calculated throughout the survey.	POSPac MMS v9
Resolve exterior orientation (EO) for each image event with omega, phi, and kappa.	POSPac MMS v9
Convert raw imagery data into geometrically corrected TIFF images.	iX Capture v3.4
Apply EO to photos and perform aerial triangulation using automatically generated tie points and ground control data.	Inpho Match AT v14
Import DEM and orthorectify image frames	Inpho OrthoMaster v14
Mosaic orthorectified imagery blending automated and manually drawn seams between photos and applying global color balancing to the project.	Inpho OrthoVista/SeamEditor v14
Resolve GPS kinematic corrections for the aircraft position data using kinematic aircraft GPS (collected at 2 Hz) and Applanix PPRTX data.	POSPac MMS v9

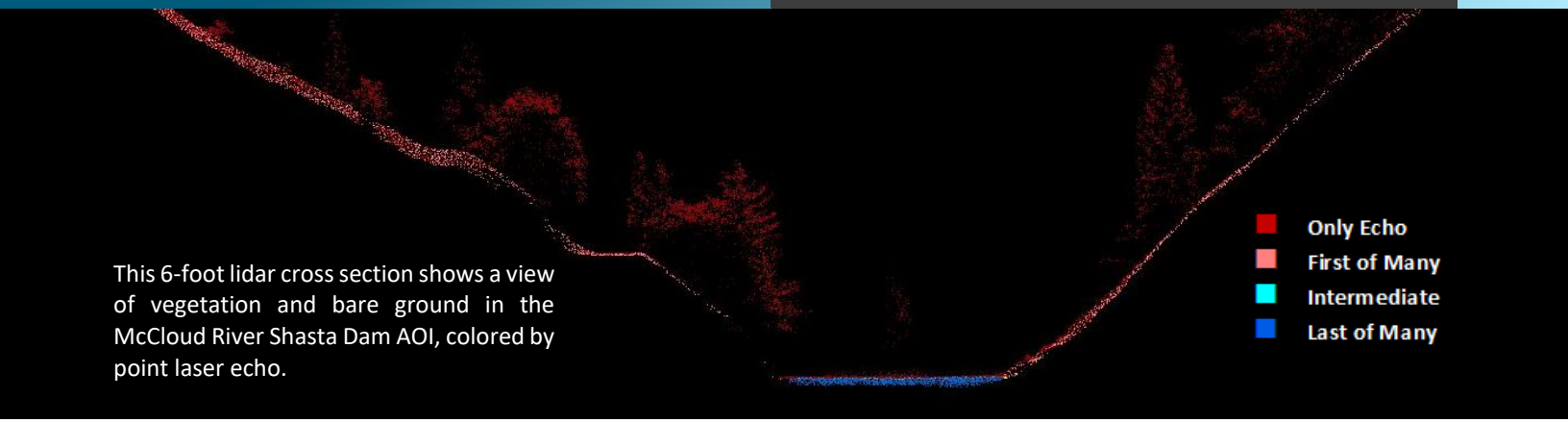

This 6-foot lidar cross section shows a view of vegetation and bare ground in the McCloud River Shasta Dam AOI, colored by point laser echo.

Bathymetric Lidar

An underlying principle for collecting hydrographic lidar data is to survey near-shore areas that can be difficult to collect with other methods, such as multi-beam sonar, particularly over large areas. The capability and effectiveness of the bathymetric lidar is impacted by several parameters including depth penetrations below the water surface, bathymetric return density, and spatial accuracy.

Lidar Limitations

NV5 worked closely with Anchor QEA to identify optimal collection periods, which required some compromise between weather, high turbidity, and shallow stream conditions. In this report, NV5 was fairly successful (mapping about 50.20% of the bathymetric areas) in acquiring most of the rivers and streams. The shallow stream flow conditions and weather combined with the altitude required to safely fly over the river may have limited the performance of the bathymetric sensors. This, along with a flight altitude of 1,300 meters for crew safety due to terrain in these areas, possibly led to a lower bathymetric coverage than what was expected for the two northern AOIs.

Lidar Point Density

First Return Point Density

The acquisition parameters were designed to acquire an average first-return density of 8 points/m^2 (0.74 points/ft^2). First return density describes the density of pulses emitted from the laser that return at least one echo to the system. Multiple returns from a single pulse were not considered in first return density analysis. Some types of surfaces (e.g., breaks in terrain, water, and steep slopes) may have returned fewer pulses than originally emitted by the laser.

First returns typically reflect off the highest feature on the landscape within the footprint of the pulse. In forested or urban areas, the highest feature could be a tree, building, or power line, while in areas of unobstructed ground, the first return will be the only echo and represents the bare earth surface.

The average first-return density of the McCloud River Shasta Dam Lidar project was 3.78 points/ft^2 (40.64 points/m^2) (Table 14). The statistical and spatial distributions of all first return densities per 100 m x 100 m cell are portrayed in Figure 9 and Figure 12.

Bathymetric and Ground Classified Point Densities

The density of ground classified lidar returns and bathymetric bottom returns were also analyzed for this project. Terrain character, land cover, and ground surface reflectivity all influenced the density of ground surface returns. In vegetated areas, fewer pulses may have penetrated the canopy, resulting in lower ground density. Similarly, the density of bathymetric bottom returns was influenced by turbidity, depth, and bottom surface reflectivity. In turbid areas, fewer pulses may have penetrated the water surface, resulting in lower bathymetric density.

The ground and bathymetric bottom classified density of lidar data for the McCloud River Shasta Dam project was 1.61 points/ft^2 (17.34 points/m^2) (Table 14). The statistical and spatial distributions per 100 m x 100 m cell of the ground and bathymetric bottom classified return densities are portrayed in Figure 10 and Figure 11.

Additionally, for the McCloud River Shasta Dam project, density values of only bathymetric bottom returns were calculated for areas containing at least one bathymetric bottom return. Areas lacking bathymetric returns (voids) were not considered in calculating an average density value. Within the successfully mapped area, a bathymetric bottom return density of 0.94 points/ft^2 (10.11 points/m^2) was achieved.

Table 14: Average Lidar point densities

Density Type	Point Density
First Returns	3.78 points/ft² 40.64 points/m²
Ground and Bathymetric Bottom Classified Returns	1.61 points/ft² 17.34 points/m²
Bathymetric Bottom Classified Returns	0.94 points/ft² 10.11 points/m²

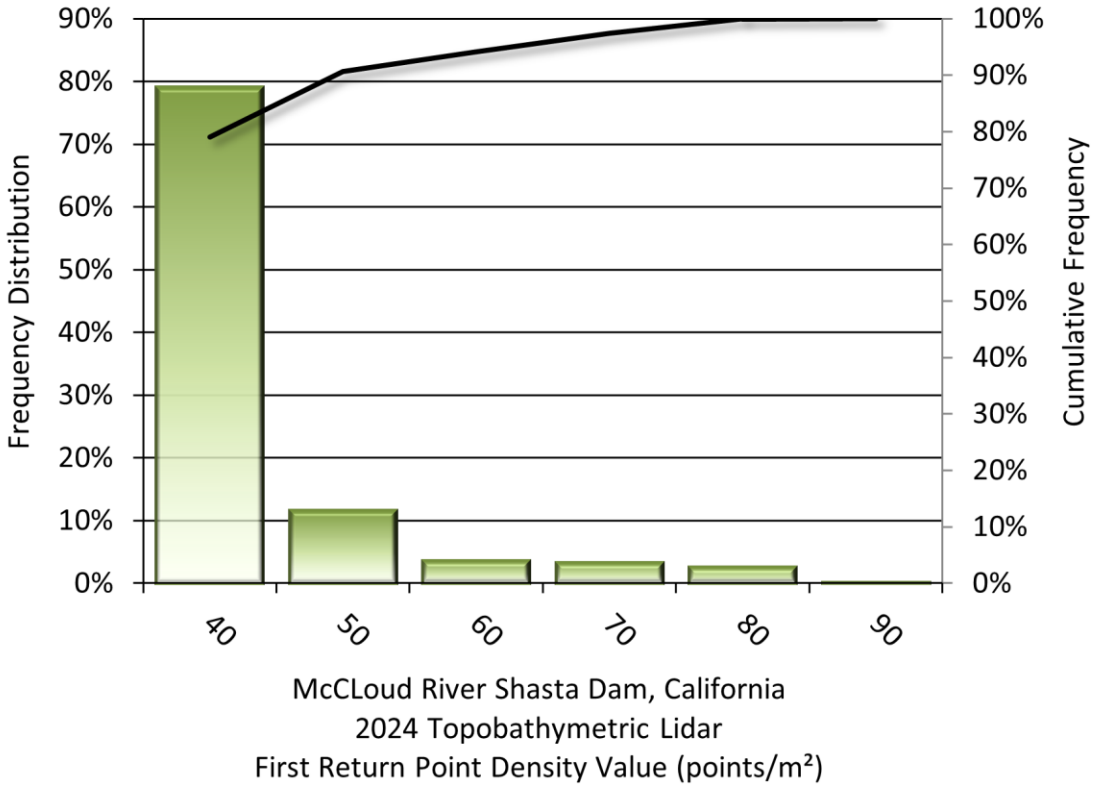

Figure 9: Frequency distribution of first return densities per 100 x 100 m cell

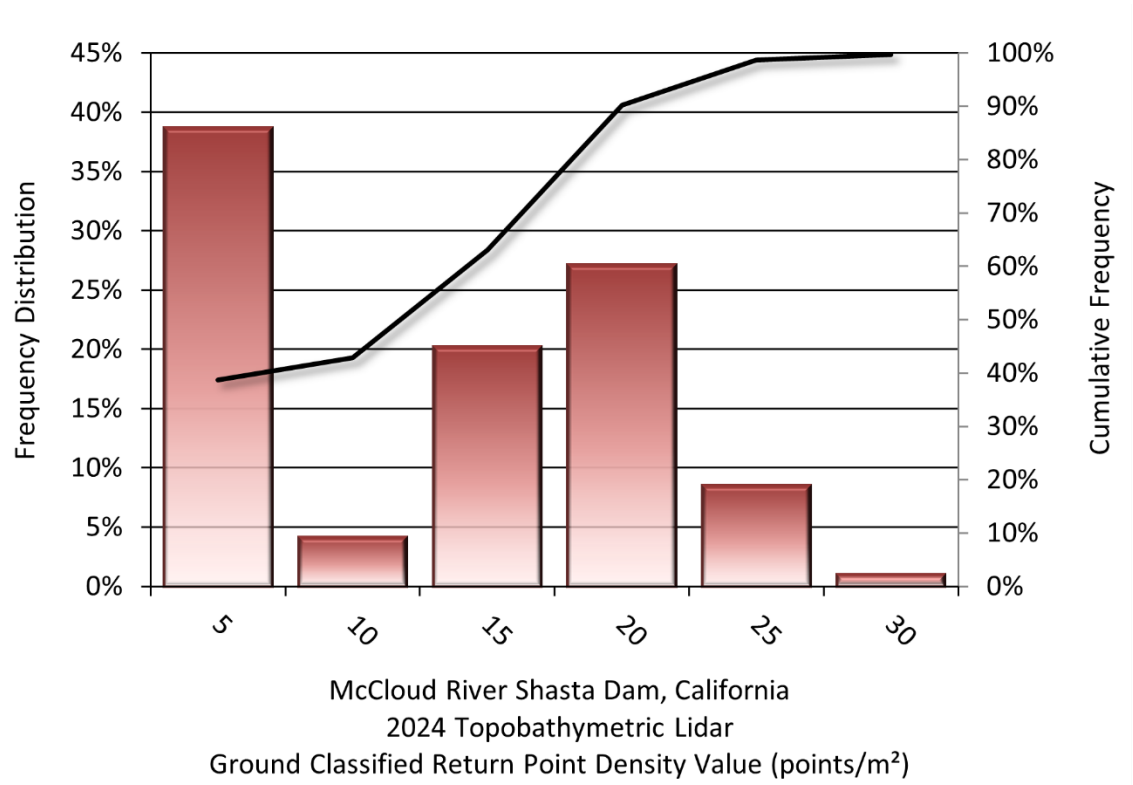

Figure 10: Frequency distribution of ground and bathymetric bottom classified return densities per 100 x 100 m cell

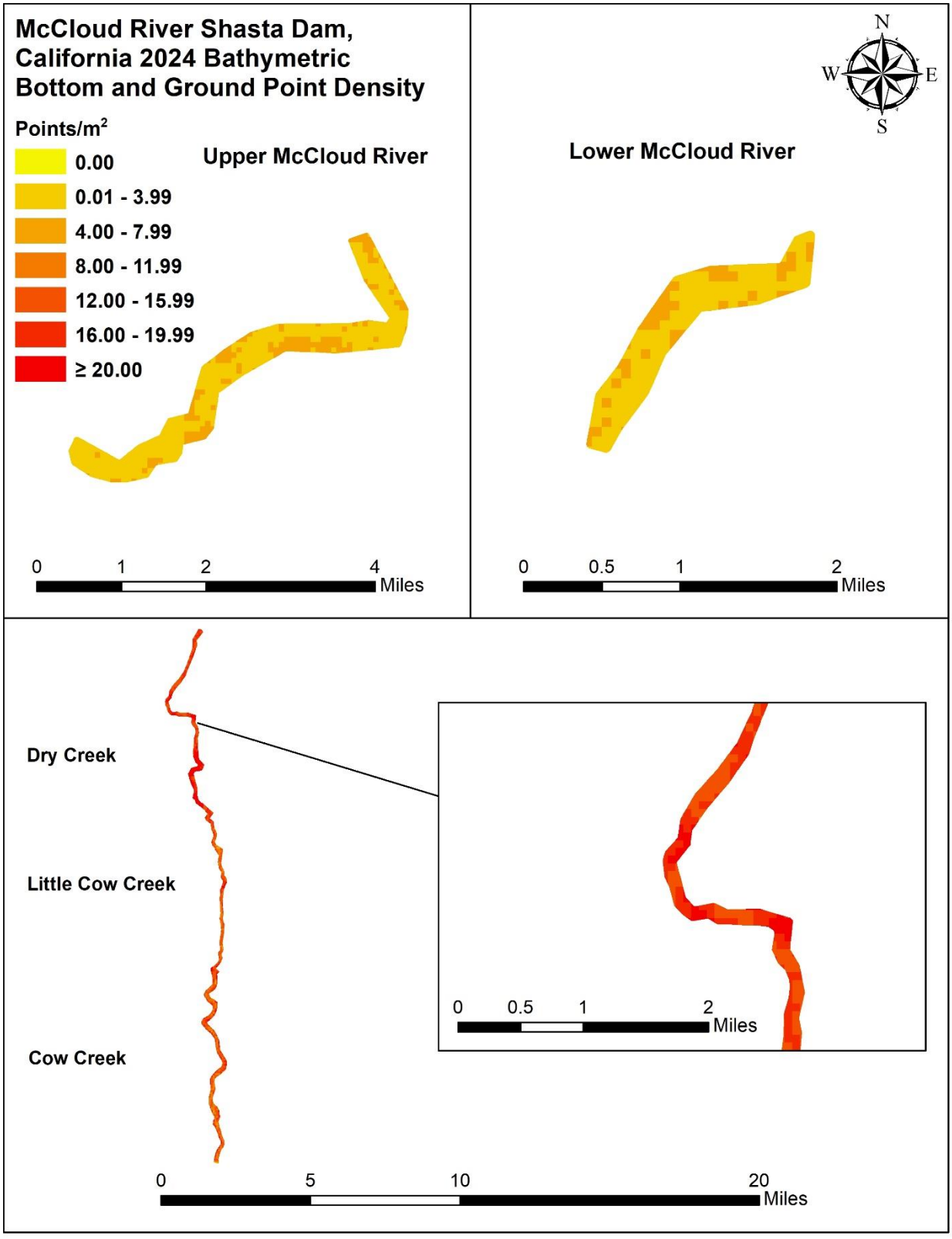

Figure 11: Ground and bathymetric bottom density map for the McCloud River Shasta Dam site (100 m x 100 m cells)

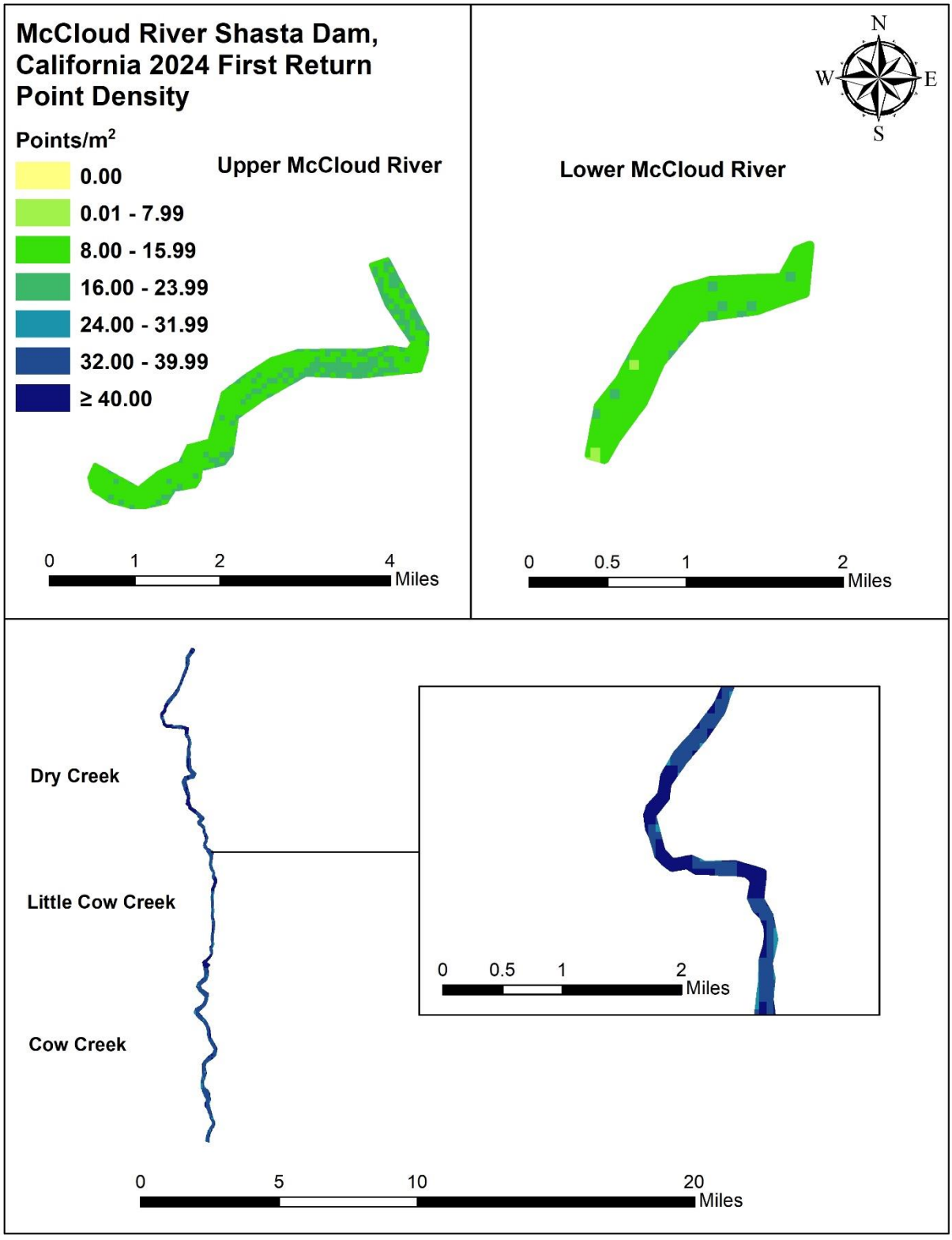

Figure 12: First Return density map for McCloud River Shasta Dam site (100 m x 100 m cells)

Lidar Accuracy Assessments

The accuracy of the lidar data collection can be described in terms of absolute accuracy (the consistency of the data with external data sources) and relative accuracy (the consistency of the dataset with itself). See Appendix A for further information on sources of error and operational measures used to improve relative accuracy.

Lidar Non-Vegetated Vertical Accuracy

Absolute accuracy was assessed using Non-vegetated Vertical Accuracy (NVA) reporting designed to meet guidelines presented in the FGDC National Standard for Spatial Data Accuracy. NVA is a measure of the accuracy of lidar point data in open areas where the lidar system has a high probability of measuring the ground surface and is evaluated at the 95% confidence interval (1.96 * RMSE), as shown in Table 15.

The mean and standard deviation (sigma σ) of divergence of the ground surface model from ground check point coordinates are also considered during accuracy assessment. These statistics assume the error for x, y and z is normally distributed, and therefore the skew and kurtosis of distributions are also considered when evaluating error statistics. For the McCloud River Shasta Dam survey, 22 ground checkpoints were withheld from the calibration and post-processing of the lidar point cloud, with resulting non-vegetated vertical accuracy of 0.191 feet (0.058 meters) as compared to the classified LAS, and 0.215 feet (0.065 meters) against the bare earth DEM, with 95% confidence (Figure 13 and Figure 14).

NV5 also assessed absolute accuracy using 174 ground control points. Although these points were used in the calibration and post-processing of the lidar point cloud, they still provide a good indication of the overall accuracy of the lidar dataset, and therefore have been provided in Table 15 and Figure 15.

Table 15: Absolute accuracy results

Parameter	NVA, as compared to Classified LAS	NVA, as compared to Bare Earth DEM	Ground Control Points
Sample	22 points	22 points	174 points
95% Confidence (1.96*RMSE)	0.191 ft 0.058 m	0.215 ft 0.065 m	0.162 ft 0.049 m
Average	0.027 ft 0.008 m	0.030 ft 0.009 m	0.018 ft 0.005 m
Median	-0.007 ft -0.002 m	0.008 ft 0.002 m	0.010 ft 0.003 m
RMSE	0.097 ft 0.030 m	0.109 ft 0.033 m	0.082 ft 0.025 m
Standard Deviation (1σ)	0.095 ft 0.029 m	0.108 ft 0.033 m	0.081 ft 0.025 m

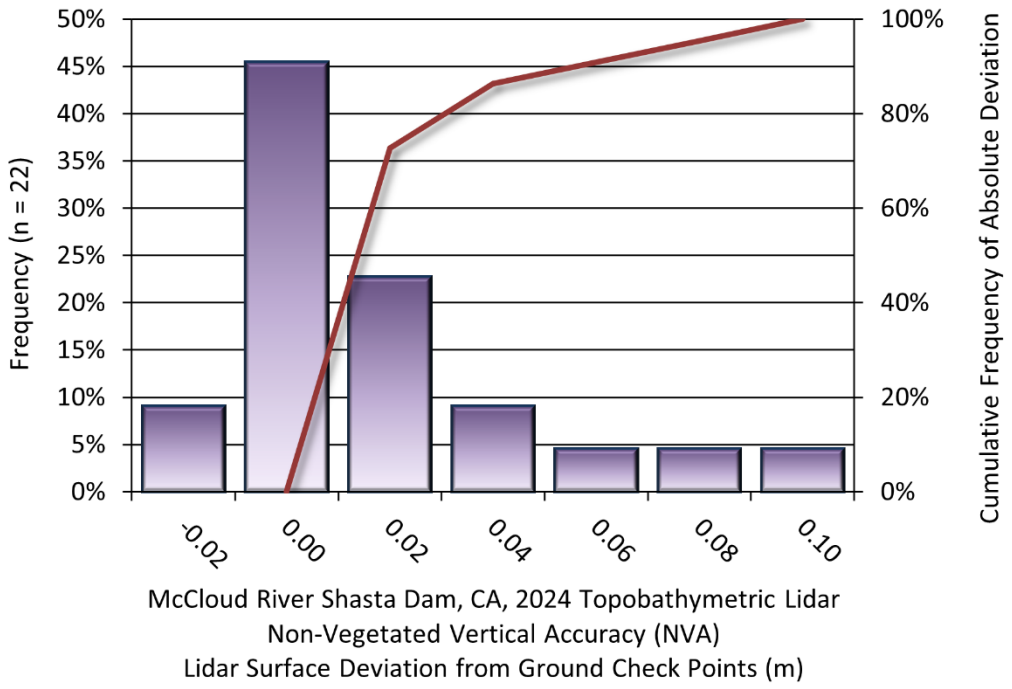

Figure 13: Frequency histogram for classified LAS deviation from ground check point values

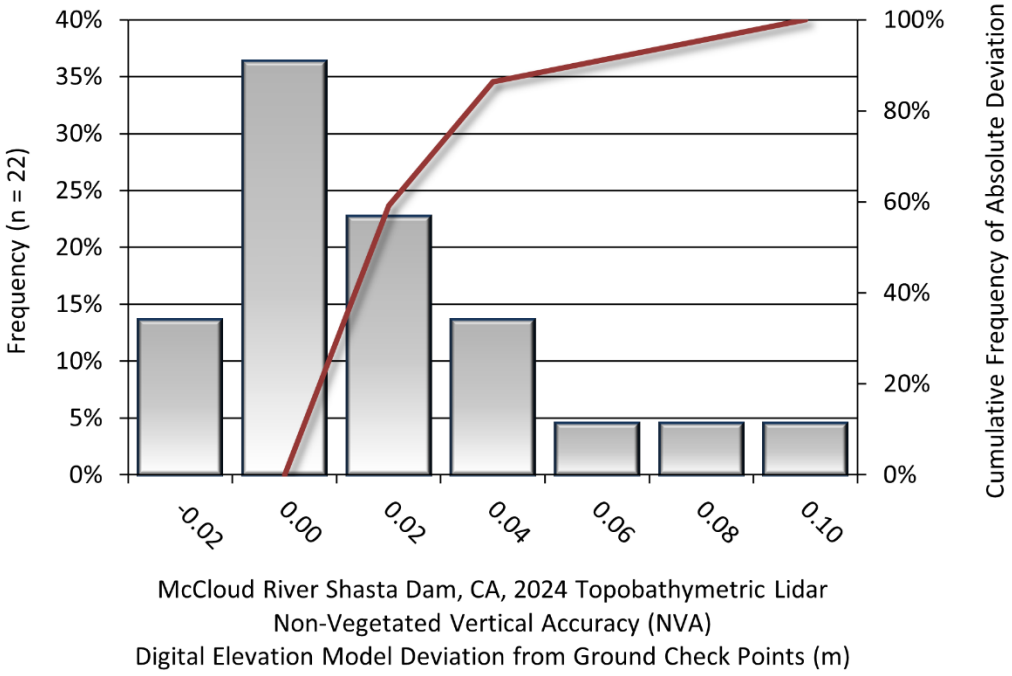

Figure 14: Frequency histogram for lidar bare earth DEM deviation from ground check point values

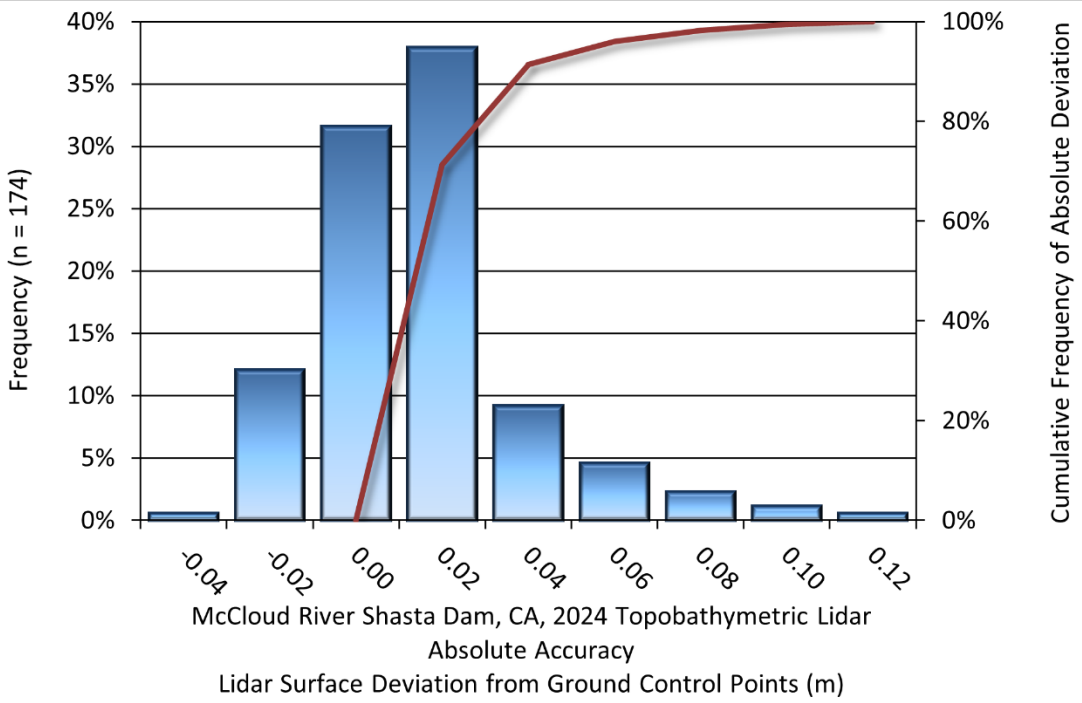

Figure 15: Frequency histogram for lidar surface deviation ground control point values

Lidar Bathymetric Vertical Accuracies

Bathymetric (submerged or along the water's edge) checkpoints were also collected in order to assess the submerged surface vertical accuracy. Assessment of 24 submerged bathymetric checkpoints resulted in a vertical accuracy of 0.138 feet (0.042 meters), while assessment of 22 wetted edge checkpoints resulted in a vertical accuracy of 0.517 feet (0.157 meters), evaluated at 95% confidence interval (Table 16, Figure 16, and Figure 17).

Table 16: Bathymetric vertical accuracy for the McCloud River Shasta Dam project

Parameter	Submerged Bathymetric Checkpoints	Wetted Edge Bathymetric Checkpoints
Sample	24 points	22 points
95% Confidence (1.96*RMSE)	0.138 ft 0.042 m	0.517 ft 0.157 m
Average Dz	0.016 ft 0.005 m	0.045 ft 0.014 m
Median	0.025 ft 0.008 m	-0.023 ft -0.007 m
RMSE	0.070 ft 0.021 m	0.264 ft 0.080 m
Standard Deviation (1σ)	0.070 ft 0.021 m	0.266 ft 0.081 m

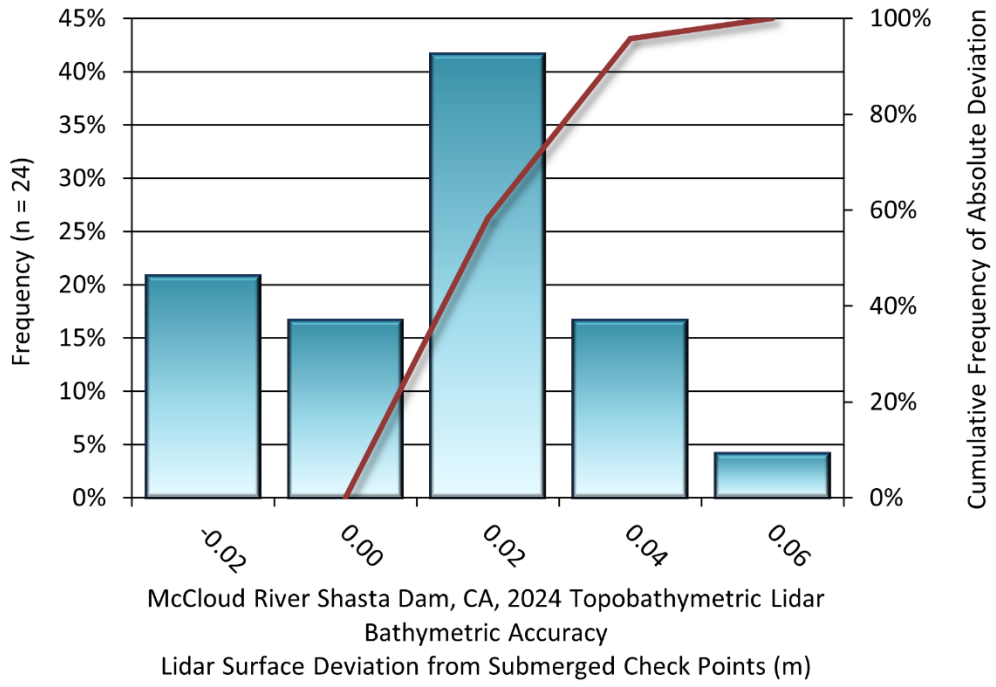

Figure 16: Frequency histogram for lidar surface deviation from submerged check point values

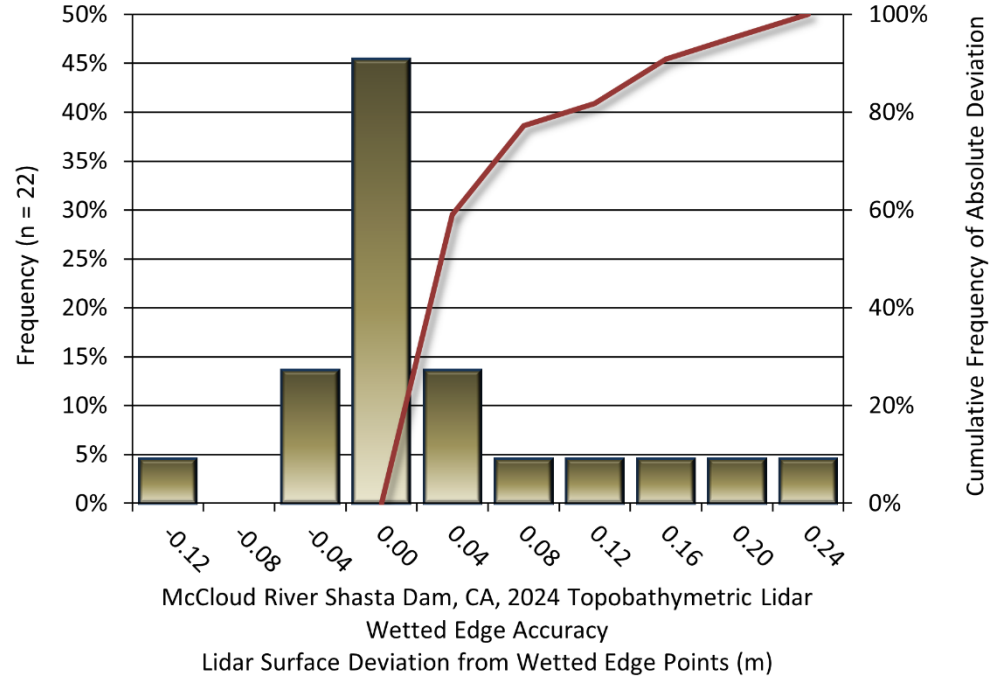

Figure 17: Frequency histogram for lidar surface deviation from wetted edge check point values

Lidar Relative Vertical Accuracy

Relative vertical accuracy refers to the internal consistency of the data set as a whole: the ability to place an object in the same location given multiple flight lines, GPS conditions, and aircraft attitudes. When the lidar system is well calibrated, the swath-to-swath vertical divergence is low (<0.10 meters). The relative vertical accuracy was computed by comparing the ground surface model of each individual flight line with its neighbors in overlapping regions. The average (mean) line to line relative vertical accuracy for the McCloud River Shasta Dam Lidar project was 0.063 feet (0.019 meters) (Table 17, Figure 18).

Table 17: Relative accuracy results

Parameter	Relative Accuracy
Sample	154 surfaces
Average	0.063 ft 0.019 m
Median	0.066 ft 0.020 m
RMSE	0.115 ft 0.035 m
Standard Deviation (1σ)	0.062 ft 0.019 m
1.96σ	0.122 ft 0.037 m

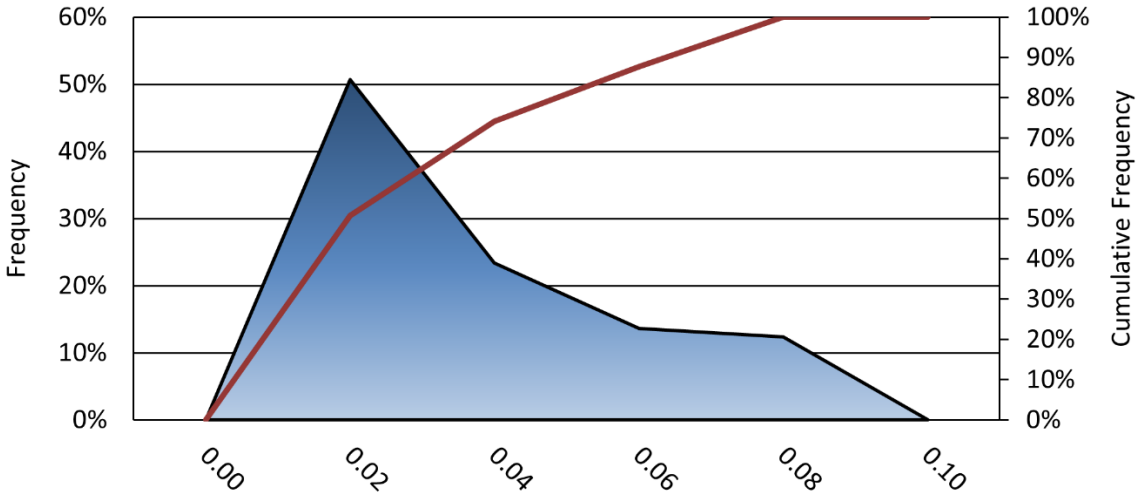

Figure 18: Frequency plot for relative vertical accuracy between flight lines

Lidar Horizontal Accuracy

Lidar horizontal accuracy is a function of Global Navigation Satellite System (GNSS) derived positional error, flying altitude, and inertial navigation system (INS) derived attitude error. The obtained $RMSE_r$ value is multiplied by a conversion factor of 1.7308 to yield the horizontal component of the National Standards for Spatial Data Accuracy (NSSDA) reporting standard where a theoretical point will fall within the obtained radius 95 percent of the time. Based on a flying altitude of 1300 meters, an IMU error of 0.002 decimal degrees, and a GNSS positional error of 0.023 meters, this project was produced to meet 0.479 feet (0.146 meters) horizontal accuracy at the 95% confidence level (Table 18).

Table 18: Horizontal accuracy

Parameter	Horizontal Accuracy
$RMSE_r$	0.277 ft 0.084 m
ACC_r	0.479 ft 0.146 m

Digital Imagery Accuracy Assessment

Image accuracy was assessed using a subset of air target points withheld from the aerial triangulation procedure as checkpoints. These points were found in the adjusted orthophotos and the displacement was recorded for further statistical analysis. Some air targets were located outside the footprint of the final orthophoto products and thus were omitted from the accuracy assessment.

This data set was tested as required by ASPRS Positional Accuracy Standards for Digital Geospatial Data, Edition 2 (2023). Although the Standards call for a minimum of thirty (30) checkpoints, this test was performed using only 6 checkpoints. This data set was produced to meet a 2 (ft) $RMSE_H$ horizontal positional accuracy class. The tested horizontal positional accuracy was found to be $RMSE_H$ = 0.168 (ft) using the reduced number of checkpoints. Table 19 presents the complete photo accuracy statistics.

Table 19: Orthophotography accuracy statistics for McCloud River Shasta Dam

Parameter	Check Points$_x$	Check Points$_y$	Check Points$_h$	Control Points$_x$	Control Points$_y$	Control Points$_h$
		n=6			n=12	
Average	-0.011 ft -0.003 m	0.005 ft 0.001 m	0.011 ft 0.004 m	0.025 ft 0.007 m	0.024 ft 0.007 m	0.034 ft 0.010 m
RMSE	0.104 ft 0.032 m	0.132 ft 0.040 m	0.168 ft 0.051 m	0.112 ft 0.034 m	0.109 ft 0.033 m	0.157 ft 0.048 m
Standard Deviation (1σ)	0.113 ft 0.035 m	0.144 ft 0.044 m	0.184 ft 0.056 m	0.114 ft 0.035 m	0.111 ft 0.034 m	0.160 ft 0.049 m
1.96σ	0.222 ft 0.068 m	0.283 ft 0.086 m	0.360 ft 0.110 m	0.224 ft 0.068 m	0.218 ft 0.067 m	0.313 ft 0.095 m
Max Error	0.072 ft 0.022 m	0.196 ft 0.060 m	0.209 ft 0.064 m	0.232 ft 0.071 m	0.235 ft 0.072 m	0.330 ft 0.101 m
Min Error	-0.174 ft -0.053 m	-0.211 ft -0.064 m	-0.273 ft -0.083 m	-0.172 ft -0.052 m	-0.161 ft -0.049 m	-0.236 ft -0.072 m

CERTIFICATIONS

NV5 provided lidar services for the McCloud River Shasta Dam project as described in this report.

I, Neil Pinto, have reviewed the attached report for completeness and hereby state that it is a complete and accurate report of this project.

Neil Pinto (Jan 6, 2025 12:07 EST) Jan 6, 2025

Neil Pinto
Project Manager
NV5

I, Evon P. Silvia, PLS, being duly registered as a Professional Land Surveyor in and by the state of California, hereby certify that the methodologies, static GNSS occupations used during airborne flights, and ground survey point collection were performed using commonly accepted Standard Practices. Field work conducted for this report was conducted on October 6-9, 2024.

Accuracy statistics shown in the Accuracy Section of this Report have been reviewed by me and found to meet the "National Standard for Spatial Data Accuracy".

Evon P. Silvia Jan 3, 2025

Evon P. Silvia, PLS
NV5
Corvallis, OR 97330

Signed: Jan 3, 2025

GLOSSARY

1-sigma (σ) Absolute Deviation: Value for which the data are within one standard deviation (approximately 68th percentile) of a normally distributed data set.

1.96 * RMSE Absolute Deviation: Value for which the data are within two standard deviations (approximately 95th percentile) of a normally distributed data set, based on the FGDC standards for Non-vegetated Vertical Accuracy (NVA) reporting.

Accuracy: The statistical comparison between known (surveyed) points and laser points. Typically measured as the standard deviation (sigma σ) and root mean square error (RMSE).

> **Absolute Accuracy:** The vertical accuracy of lidar data is described as the mean and standard deviation (sigma σ) of divergence of lidar point coordinates from ground survey point coordinates. To provide a sense of the model predictive power of the dataset, the root mean square error (RMSE) for vertical accuracy is also provided. These statistics assume the error distributions for x, y and z are normally distributed, and thus we also consider the skew and kurtosis of distributions when evaluating error statistics.
>
> **Relative Accuracy:** Relative accuracy refers to the internal consistency of the data set; i.e., the ability to place a laser point in the same location over multiple flight lines, GPS conditions and aircraft attitudes. Affected by system attitude offsets, scale and GPS/IMU drift, internal consistency is measured as the divergence between points from different flight lines within an overlapping area. Divergence is most apparent when flight lines are opposing. When the lidar system is well calibrated, the line-to-line divergence is low (<10 cm).
>
> **Root Mean Square Error (RMSE):** A statistic used to approximate the difference between real-world points and the lidar points. It is calculated by squaring all the values, then taking the average of the squares and taking the square root of the average.

Data Density: A common measure of lidar resolution, measured as points per square meter.

Digital Elevation Model (DEM): File or database made from surveyed points, containing elevation points over a contiguous area. Digital terrain models (DTM) and digital surface models (DSM) are types of DEMs. DTMs consist solely of the bare earth surface (ground points), while DSMs include information about all surfaces, including vegetation and man-made structures.

Intensity Values: The peak power ratio of the laser return to the emitted laser, calculated as a function of surface reflectivity.

Nadir: A single point or locus of points on the surface of the earth directly below a sensor as it progresses along its flight line.

Overlap: The area shared between flight lines, typically measured in percent. 100% overlap is essential to ensure complete coverage and reduce laser shadows.

Pulse Rate (PR): The rate at which laser pulses are emitted from the sensor; typically measured in thousands of pulses per second (kHz).

Pulse Returns: For every laser pulse emitted, the number of wave forms (i.e., echoes) reflected back to the sensor. Portions of the wave form that return first are the highest element in multi-tiered surfaces such as vegetation. Portions of the wave form that return last are the lowest element in multi-tiered surfaces.

Real-Time Kinematic (RTK) Survey: A type of surveying conducted with a GPS base station deployed over a known monument with a radio connection to a GPS rover. Both the base station and rover receive differential GPS data and the baseline correction is solved between the two. This type of ground survey is accurate to 1.5 cm or less.

Post-Processed Kinematic (PPK) Survey: GPS surveying is conducted with a GPS rover collecting concurrently with a GPS base station set up over a known monument. Differential corrections and precisions for the GNSS baselines are computed and applied after the fact during processing. This type of ground survey is accurate to 1.5 cm or less.

Scan Angle: The angle from nadir to the edge of the scan, measured in degrees. Laser point accuracy typically decreases as scan angles increase.

Native Lidar Density: The number of pulses emitted by the lidar system, commonly expressed as pulses per square meter.

Relative Accuracy Calibration Methodology:

Manual System Calibration: Calibration procedures for each mission require solving geometric relationships that relate measured swath-to-swath deviations to misalignments of system attitude parameters. Corrected scale, pitch, roll and heading offsets were calculated and applied to resolve misalignments. The raw divergence between lines was computed after the manual calibration was completed and reported for each survey area.

Automated Attitude Calibration: All data was tested and calibrated using TerraMatch automated sampling routines. Ground points were classified for each individual flight line and used for line-to-line testing. System misalignment offsets (pitch, roll and heading) and scale were solved for each individual mission and applied to respective mission datasets. The data from each mission were then blended when imported together to form the entire area of interest.

Automated Z Calibration: Ground points per line were used to calculate the vertical divergence between lines caused by vertical GPS drift. Automated Z calibration was the final step employed for relative accuracy calibration.

Lidar accuracy error sources and solutions:

Source	Type	Post Processing Solution
Long Base Lines	GPS	None
Poor Satellite Constellation	GPS	None
Poor Antenna Visibility	GPS	Reduce Visibility Mask
Poor System Calibration	System	Recalibrate IMU and sensor offsets/settings
Inaccurate System	System	None
Poor Laser Timing	Laser Noise	None
Poor Laser Reception	Laser Noise	None
Poor Laser Power	Laser Noise	None
Irregular Laser Shape	Laser Noise	None

Operational measures taken to improve relative accuracy:

Focus Laser Power at narrow beam footprint: A laser return must be received by the system above a power threshold to accurately record a measurement. The strength of the laser return (i.e., intensity) is a function of laser emission power, laser footprint, flight altitude and the reflectivity of the target. While surface reflectivity cannot be controlled, laser power can be increased and low flight altitudes can be maintained.

Reduced Scan Angle: Edge-of-scan data can become inaccurate. The scan angle was reduced to a maximum of ±20˚ to ±21° for the green and NIR lasers, respectively, from nadir, creating a narrow swath width and greatly reducing laser shadows from trees and buildings.

Quality GPS: Flights took place during optimal GPS conditions (e.g., 6 or more satellites and PDOP [Position Dilution of Precision] less than 3.0). Before each flight, the PDOP was determined for the survey day.

Ground Survey: Ground survey point accuracy (<1.5 cm RMSE) occurs during optimal PDOP ranges and targets a minimal baseline distance of 4 miles between GPS rover and base. Robust statistics are, in part, a function of sample size (n) and distribution. Ground survey points are distributed to the extent possible throughout multiple flight lines and across the survey area.

50% Side-Lap (100% Overlap): Overlapping areas are optimized for relative accuracy testing. Laser shadowing is minimized to help increase target acquisition from multiple scan angles. Ideally, with a 50% side-lap, the nadir portion of one flight line coincides with the swath edge portion of overlapping flight lines. A minimum of 50% side-lap with terrain-followed acquisition prevents data gaps.

Opposing Flight Lines: All overlapping flight lines have opposing directions. Pitch, roll and heading errors are amplified by a factor of two relative to the adjacent flight line(s), making misalignments easier to detect and resolve.